Cardiovascular Research (2013) **97**, 533–543
doi:10.1093/cvr/cvs369

Induction of oxidative stress by oxidized LDL via meprinα-activated epidermal growth factor receptor in macrophages

Pan Gao[1], Xiao-mei Wang[1], Dei-hui Qian[2], Ze-Xue Qin[2], Jun Jin[2], Qiang Xu[1], Qiao-Ying Yuan[1], Xue-Jun Li[1], and Liang-Yi Si[1]*

[1]Chongqing Key Disciplines, Department of Geriatrics, Southwest Hospital, Third Military Medical University, Chongqing 400038, China; and [2]Institute of Cardiovascular Science, Xinqiao Hospital, Third Military Medical University, Chongqing 400037, China

Received 19 July 2012; revised 20 November 2012; accepted 10 December 2012; online publish-ahead-of-print 17 December 2012

Time for primary review: 46 days

Aims The aim of this study was to explore meprinα-mediated transactivation of the epidermal growth factor receptor (EGFR) and reactive oxygen species (ROS) production in macrophages.

Methods and results Accelerated atherosclerotic lesions were established by administration of a high-fat diet in apolipoprotein E-deficient (apoE$^{-/-}$) mice. Lentiviral overexpression of meprinα in the thoracic aortic artery during plaque formation enhanced intra-plaque macrophage induction of ROS as well as formation of atherosclerotic plaques, whereas AG1478 (specific inhibitor of the EGFR) treatment exerted the opposite effect. A meprinα inhibitor abrogated EGFR activation in mice. In cultured J774a.1 macrophages, oxidized low-density lipoprotein (OxLDL) increased ROS formation and EGFR activation through a ligand [heparin-binding epidermal growth factor-like growth factor (HB-EGF)]-dependent pathway. However, a meprinα inhibitor or specific siRNA inhibited ROS production and EGFR activation. Recombinant mouse meprinα enhanced OxLDL-stimulated production of ROS and induced HB-EGF. Inhibition of p38 mitogen-activated protein kinase by SB203580 decreased OxLDL-stimulated production of ROS. Conversely, inhibition of meprinα or PI3K-Rac1 inhibitors also decreased p38 activity in OxLDL-stimulated macrophages. In addition, inhibition of meprinα reversed OxLDL-stimulated activation of PI3K.

Conclusion Meprinα promotes OxLDL-induced plaque formation and ROS release by transactivation of the EGFR, followed by activation of the PI3K/Rac1/p38 pathway.

Keywords Atherosclerosis • Reactive oxygen species • Epidermal growth factor receptor • Meprin • Oxidized low density lipoprotein

1. Introduction

Oxidized low-density lipoprotein (OxLDL) is a major pathogenic factor in the development of atherosclerosis.[1] Increased intracellular formation of reactive oxygen species (ROS) plays a critical part in OxLDL-induced formation of atherosclerotic plaques,[2,3] but the mechanism is incompletely understood. Studies have identified (at least in part) the intracellular signalling pathway regulated by OxLDL. Accumulated evidences showed that OxLDL can induce ROS production and release inflammatory factors via 'scavenger receptors'.[4,5] Besides scavenger receptors, another receptor of interest which OxLDL has been shown to transactivate is the epidermal growth factor receptor (EGFR).[6–8] The EGFR plays a key part in many cellular processes, and is important for ROS production and the release of inflammatory mediators from macrophages.[9,10] Activation of the EGFR leads to downstream activation of mitogen-activated protein kinases (MAPKs) such as p38 (stress activated), NH_2-terminal c-Jun kinase (JNK), extracellular signal-regulated kinase (ERK) 1 and ERK 2, and protein kinase B/Akt.[11] Once activated, these kinases are translocated to the nucleus, where they bind to and phosphorylate nuclear transcription factors, stimulating gene transcription, protein synthesis, and cell growth.[12,13] The EGFR is a transmembrane protein consisting of an extracellular ligand-binding domain to which EGFR ligands bind for activation.[14] In addition to direct activation by

* Corresponding author. Tel: +86 23 68754150; Fax: +86 23 68754150, Email: doctorsly@126.com

EGFR ligands, the EGFR can also be transactivated by other stimulus. In at least some instances, transactivation of the EGFR occurs through an extracellular pathway that is dependent upon the activity of members of the metalloproteinase family, which induce the shedding of growth factors [e.g. heparin-binding epidermal growth factor (HB-EGF)] and thereby transactivation of the EGFR.[15–17]

Meprins were discovered to be membrane-bound metalloproteinase in the kidneys of mice. Meprins consist of two subunits (α and β) which form disulfide-bridged homodimers and heterodimers that differ in oligomerization potentials and substrate specificity.[18] Accumulated evidences have demonstrated that meprins are implicated in inflammation. For example, they participate in the: progression of intestinal inflammation;[19] altered homeostasis of monocytes and natural killer cells:[20] enhanced production of inflammatory factors in mononuclear cells.[21]

Actinonin is a specific inhibitor of α subunit of meprin. Actinonin is a much more potent inhibitor of the activity of meprinα than meprinβ. Actinonin might therefore be a lead compound for the development of selective, subunit-specific inhibitors.[18] We recently found that actinonin reduced production of ROS in macrophages, and also suppressed formation of atherosclerosis in apoE$^{-/-}$ mice fed a high-fat diet.[22] Studies have also shown that meprinα transactivates the EGFR in epithelial cells, but that meprinα-mediated transactivation of the EGFR is dependent upon different ligands if cells contain neutrophil elastase[23] or haem.[24] However, the link between meprinα and OxLDL signalling has not been elucidated.

In the present study, we tried to ascertain whether meprinα-mediated transactivation of the EGFR is involved in OxLDL-induced ROS production. We subsequently investigated the pathway of meprinα-mediated transactivation of the EGFR under stimulation of OxLDL as well as their downstream signalling.

2. Methods

2.1 Reagents

Reagents were purchased from Sigma (St Louis, MO, USA), unless stated otherwise. Recombinant mouse meprinα was purchased from R&D Systems (Shanghai, China). OxLDL was obtained from DingGuo Biotech (Chongqing, China).

2.2 Preparation of lentivirus vectors

The viral vector was derived from the human immunodeficiency virus-based lentivirus backbone, pLV-CMV-GFP-3Flag, and was purchased from SunBio Technology (Shanghai, China). The pLV-CMV-GFP-3Flag vector allows for virally mediated expression of green fluorescent protein (GFP) driven by a cytomegalovirus (CMV) promoter. The pLV-CMV-GFP-3Flag control vector is referred to as *L-EGFP*. Murine meprinα cDNA (NM_008585.2) was amplified by a reverse transcription–polymerase chain reaction and cloned into the pLV-CMV-GFP-3Flag vector using *Eco*RI and *Age*I sites, and referred to as *L-meprinα*. The meprinα cDNA sequence was confirmed by sequencing. Recombinant viruses were packaged and amplified in HEK-293T cells and purified by anion chromatography. The titre of the viral vectors was determined using the 50% tissue culture infective dose (TCID50) method.

2.3 Animals experiments

Animal experiments were conducted in accordance with the institutional guidelines of the Third Military Medical University and the Guide for the Use and Care of Laboratory Animals, as published by the US National Institutes of Health (NIH, 8th edition, 2011). One hundred fifty 6-week-old apoE$^{-/-}$ mice (C57/Bl6 genetic background; purchased from Beijing University, China) were randomly assigned to six groups (see Supplementary material online, *Figure S1*). The **CON** group ($n = 25$) was provided a normal diet for 14 weeks; the remaining animals, maintained on the same atherogenic diet throughout the duration of the study (1% cholesterol and 20% fatty acids for 14 weeks), were randomized into five groups at the beginning of 11th week as follows: the **HF** group ($n = 25$) received an intraperitoneal injection of sterile saline (0.5 mL per day) for 4 weeks; the **HF+LM** group ($n = 25$) received an intravenous injection of L-meprinα (1.84×10^8 TU via tail vein injection) and an additional 4 weeks of intraperitoneal injections with sterile saline; the **HF+LM+AC** group ($n = 25$) received an intravenous injection of L-meprinα and an additional 4 weeks of intraperitoneal injections with actinonin (5 mg/kg/day); the **HF+LM+AG** group ($n = 25$) received an intravenous injection of L-meprinα and an additional 4 weeks of intraperitoneal injections with AG1478 [a specific EGFR inhibitor (20 mg/kg/day)]; and the **HF+LGFP** group ($n = 25$) received an intravenous injection of L-EGFP (1.92×10^8 TU). Before the injections, the mice were anaesthetized with an intraperitoneal injection of sodium pentobarbitone (40 mg/kg). Loss of reflex was detected by pricking the animal's feet and legs with forceps. The mice were then anaesthetized by an intraperitoneal injection of sodium pentobarbitone (150 mg/kg) before exsanguination by perfusion via the abdominal aorta with phosphate-buffered saline (PBS) at a constant pressure of 100 mmHg, with outflow through the incised jugular veins.

Six mice in the **HF+LGFP** group were sacrificed 1 and 4 weeks after the infection to determine the efficiency of the delivery of the lentivirus gene in atherosclerotic plaques. Cryosections were viewed on a confocal laser scanning microscope (Leica TCS SP5) to identify GFP expression. To reduce the autofluorescence, sections were pre-incubated in pontamine sky blue (0.5% wt/vol) and 2% glyoxylic acid mixed in phosphate buffer for 30 min at room temperature, followed by a 5 min wash before mounting, as previously described.[25]

2.4 Tissue preparation and histologic analyses

Six-to-nine thoracic aortas in each group were carefully excised and immersed in 4% formaldehyde overnight at 4°C, and then each vessel was cut into four to five segments. Two segments from each vessel were stored in liquid nitrogen until used in western blot assay. The remaining segments of thoracic aortas were embedded in paraffin blocks, and four to five segments in each group were embedded in one paraffin block. Serial sections were cut (6 μm thick) every 50 μm along the artery, and approximately 100 sections per vessel were obtained. Serial sections were cut (6 μm thick) every 50 μm along the artery, and approximately 100 sections per vessel were obtained. The site of maximal plaque size was stained with haematoxylin and eosin for morphologic analysis. Images were captured with a Leica microscope (Leica DMI3000 B). To determine the site of maximal plaque size in each section, the maximal plaque area was determined by Image Pro Plus 6.0 software (IPP 6.0), and the maximal plaque area in all sections was chosen as the site of maximal plaque size in the entire vessel. For *en face* analysis, six vessels in each group were excised and placed in Oil-red-O for 30 min at 37°C, and then washed with PBS. Images of artery plaques were obtained with a SONY digital camera.

2.5 Measurement of *in situ* ROS production

Oxidative stress in the aorta was determined by assessing the vascular superoxide production *in situ* using dihydroethidium (DHE, Beyotime Biotechnology) fluorescence microscopy (see Supplementary material online).

2.6 Immunohistochemistry

Sections were blocked and incubated with antibodies against p-EGFR (CST) or meprinα (Roche) overnight at 4°C, and then incubated with

biotinylated secondary antibody for 30 min and visualized with a 3,3′-diaminobenzidine (DAB) kit (see Supplementary material online).

2.7 Immunofluorescence

Cryosections were incubated with double primary antibodies, including antibodies against macrophages (CD68, Abcam) and meprinα (Santa Cruz), at 4°C overnight. Alexa Fluor 555- and 633-labelled IgG (Molecular Probes) were used as secondary antibodies. Cell nuclei were visualized with application of 4′,6-diamidino-2-phenylindole (DAPI, molecular probes; see Supplementary material online).

2.8 Cell culture and small-interfering RNA (siRNA) assay

J774A.1 macrophages were purchased from the American Type Culture Collection (ATCC). Macrophages were transfected with control or meprinα-specific siRNA(Ambion) using Lipofectamine. siRNA efficiency of protein suppression was confirmed by western blot analysis (see Supplementary material online).

2.9 Intracellular ROS production

J774A.1 cells were plated in 96-well plates in media containing 10% FBS. After incubation with OxLDL, cells were fixed with acetone, permeabilized with 0.1% Triton X-PBS, and stained with 10 μM DHE for 30 min. Cell were washed with PBS and DHE fluorescent was determined in 10 random fields per dish under a fluorescence microscope.

2.10 Enzyme-linked immunosorbent assay (ELISA)

A standard enzyme-linked immunosorbent assay (ELISA) method, as described by the manufacturer (BioSource International), was used to measure HB-EGF protein concentrations (see Supplementary material online).

2.11 Western blot analyses

Fifty micrograms of protein were separated by SDS–PAGE and transferred onto PVDF membranes, which were blocked and incubated with antibodies. Bands were detected by horseradish peroxidase-coupled secondary antibody and chemiluminescence (see Supplementary material online).

2.12 GST pull-down assay for activated Rac1

After treatment with OxLDL or with OxLDL+wortmanin, a GST pull-down assay was conducted according to the manufacturer's instructions using Rac1 activation assay kits (Thermo Scientific, see Supplementary material online).

2.13 Statistical analyses

SPSS (version 13.0) was used for statistical analyses. All experiments were repeated at least three times. Data are the mean ± SEM. Groups of data were compared with ANOVA, followed by Tukey's multiple comparison tests. Data that did not follow a normal distribution were analysed with the Mann–Whitney test or Student's *t*-test after log normalization. $P < 0.05$ was considered significant.

3. Results

3.1 Up-regulation of meprinα expression in atherosclerotic plaques

To clarify the role of meprinα in atherogenesis, we first determined the expression of meprinα in thoracic aorta plaques in ApoE$^{-/-}$ mice. Compared with the plaques in **CON** mice without atherosclerotic lesions, the level of expression of the meprinα protein was upregulated in **HF** mice measured by immunohistochemistry and western blot (*Figure 1A* and *B*).

3.2 The essential role of EGFR signalling in meprinα-promoted atherosclerosis formation

To assess the efficiency of lentiviral delivery of meprinα by intravenous injection, the GFP fluorescence of thoracic aorta plaques was observed in **LGFP** mice. Elevated GFP fluorescence was observed in plaques of **LGFP** mice 1 and 4 weeks after the infection compared with lesions in HF mice (*Figure 1C*). To characterize the expression of meprinα in intra-plaque cell types, we simultaneously stained meprinα and macrophages of thoracic aorta plaques transfected with L-EGFP or L-meprinα and showed the augmentation of meprinα expression in **HF+LM** mice; however, the expression of meprinα was not significantly increased in **HF+LGFP** mice ($P < 0.05$, *Figure 1D*, vs. **HF** mice).

We then tested whether or not meprinα-accelerated atherosclerosis is dependent upon EGFR transactivation. After administration of L-meprinα, plaque formation and DHE fluorescence were significantly higher in the **HF+LM** group than the **HF** group ($P < 0.05$, *Figures 2, 3A* and *B*). When mice were administered AG1478 or actinonin daily after injection of L-meprinα, plaque formation was significantly reversed by inhibitors ($P < 0.05$, *Figure 2*, vs. **HF+LM** mice). In addition, DHE fluorescence was also decreased in the **HF+LM+AG** group when compared with the **HF+LM** group ($P < 0.05$, *Figure 3A* and *B*). Furthermore, the expression of phosphor-EGFR was detected by immunohistochemistry. As expected, the **HF+LM** mice had higher expression of phosphor-EGFR compared with the mice in the **HF** group; however, the expression of phosphor-EGFR in **HF+LM+AC** mice was significantly reduced compared with **HF+LM** mice ($P < 0.05$, *Figure 3C* and *D*). Taken together, the effects of L-meprinα on plaque morphology and pathologic changes were reversed by a specific EGFR inhibitor.

3.3 Involvement of meprinα signalling in ROS induction by OxLDL

We then determined whether or not meprinα has an essential role in OxLDL regulation of ROS production. Pre-incubation with OxLDL for 30 min induced cellular ROS production in a dose-dependent manner ($P < 0.05$, *Figure 4A* and Supplementary material online, *Figure S2*), whereas native LDL (nLDL; 100 μg/mL for 30 min) did not induce cellular ROS production ($P > 0.05$ vs. control, *Figure 4A* and Supplementary material online, *Figure S2*). Macrophages were then pre-incubated with actinonin (100 μmol/L for 1 h) or a meprinα-specific siRNA (meprinα siRNA for 24 h), followed by incubation with OxLDL. To clarify the effects of meprinα siRNA on the expression of meprinα, western blot showed that meprinα siRNA significantly blocked the expression of meprinα (Supplementary material online, *Figure S5*). As shown in *Figure 4B* and Supplementary material online, *Figure S2*, actinonin and meprinα siRNA (100 nmol/L for 24 h) inhibited the OxLDL-mediated increase in ROS production ($P < 0.01$ vs. 100 μg/mL of OxLDL treated alone). In addition, OxLDL stimulation, after pre-incubation with recombinant mouse meprinα (50 ng/mL for 2 h), increased ROS levels in macrophages ($P < 0.01$ vs. OxLDL treated alone).

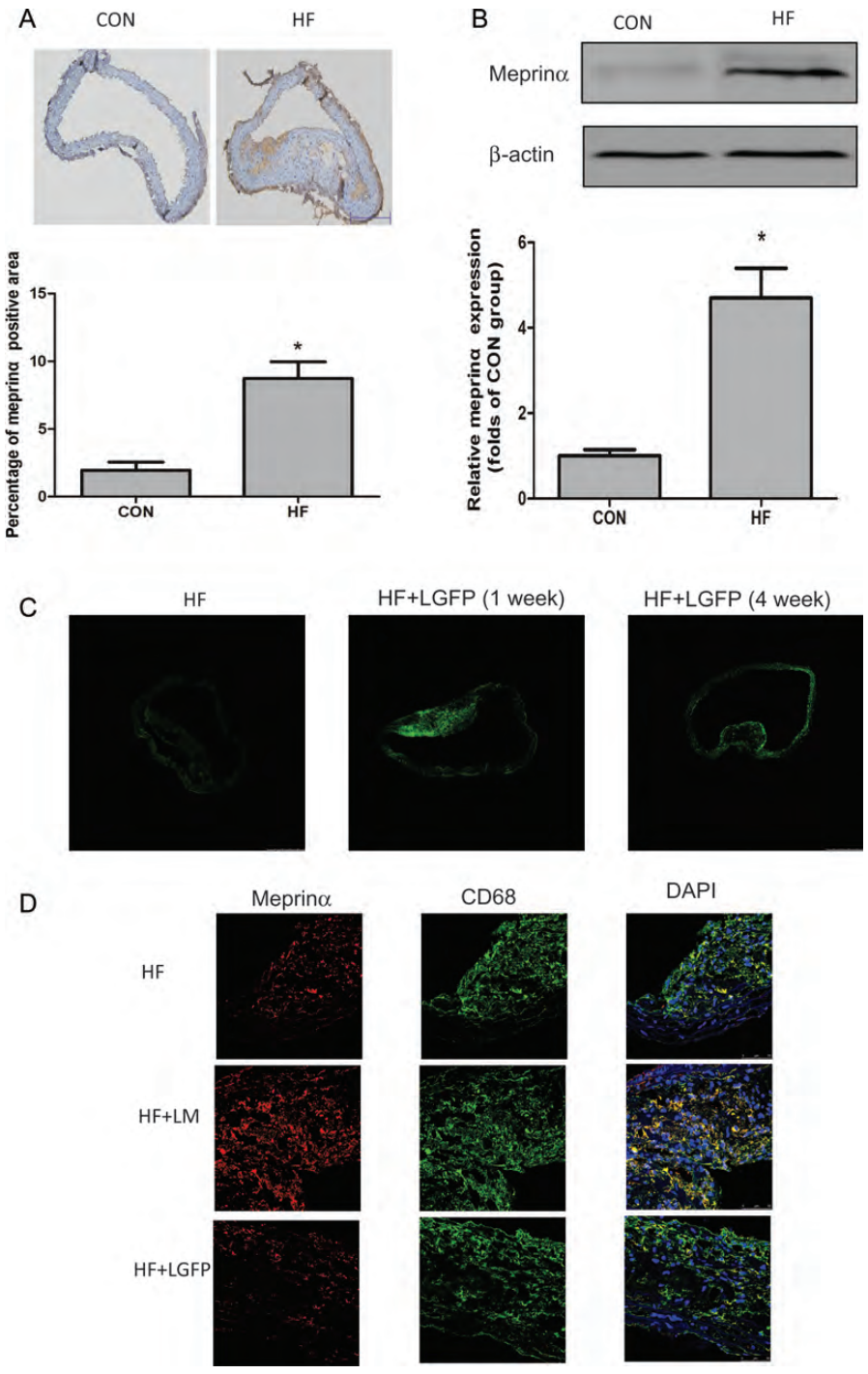

Figure 1 Up-regulation of meprinα expression in atherosclerotic plaques. (*A*) Immunohistochemical staining of meprinα in the aortic plaques of **CON** and **HF** mice. ($n = 6–9$, bar = 200 μm). The bar chart below shows the quantitative analysis of meprinα in the two groups, $^*P < 0.01$ vs. **CON**. (*B*) Level of expression of the meprinα protein in thoracic aortas of **CON** and **HF** mice by western blot. $n = 6–9$, $^*P < 0.01$ vs. **CON**. (*C*) Representative examples of eGFP-positive areas in the aortic lesions to demonstrate the efficiency of lentiviral delivery by intravenous injection in atherosclerosis ($n = 6$, bar = 250 μm). (*D*) Macrophages expressing meprinα in a plaque of different groups. Blue colour indicates macrophage nuclei; red colour depicts meprinα; green colour shows macrophages ($n = 8–10$, Bar = 25 μm).

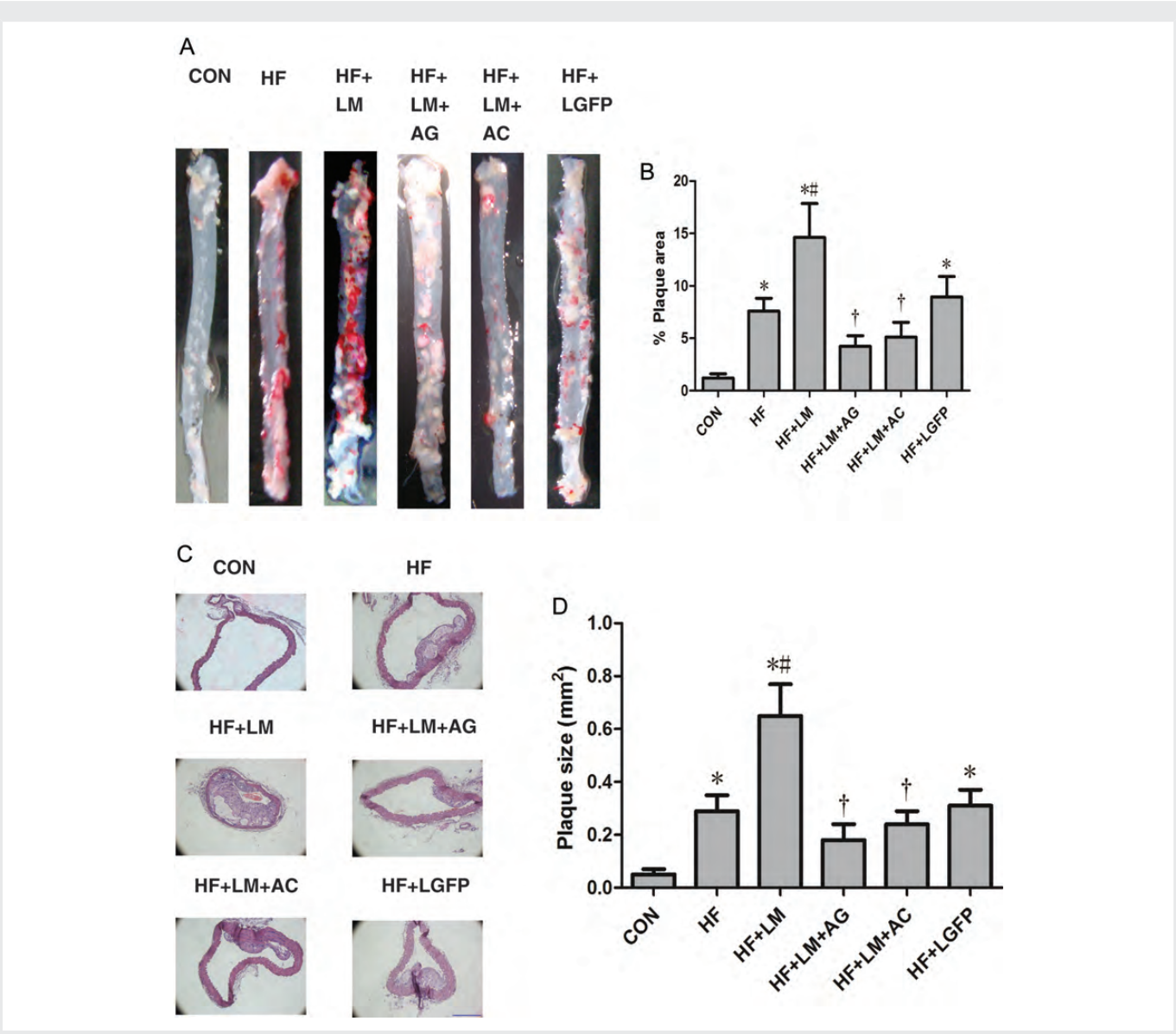

Figure 2 Regulation of atherosclerotic lesions in apoE$^{-/-}$ mice with lentiviral delivery of meprinα and administration with actinonin or AG1478. (*A* and *B*) Representative *en face* images (*A*) showing Oil red O-stained plaque areas of thoracic aortas and (*B*) percentage of plaque areas ($n = 6$). $^{*}P < 0.01$ vs. **CON,** $^{\#}P < 0.01$ vs. **HF**, and $^{\dagger}P < 0.01$ vs. **HF+LM**. (*C*) Paraffin sections of thoracic aortic plaques stained with haematoxylin and eosin ($n = 6–9$, bar = 200 μm). (*D*) Plaque areas were quantified by IPP6.0. $^{*}P < 0.01$ vs. **CON,** $^{\#}P < 0.01$ vs. **HF**, and $^{\dagger}P < 0.01$ vs. **HF+LM.**

3.4 Involvement of EGFR signalling and transactivation of EGFR by meprinα in OxLDL-mediated ROS production

To ascertain if activation of EGFR is related to the OxLDL-stimulated increase in ROS levels, macrophages were pre-incubated with AG1478 (200 nmol/L for 30 min), followed by incubation with OxLDL. As shown in *Figure 4C* and Supplementary material online, *Figure S3*, OxLDL-induced ROS production in macrophages was abolished ($P < 0.01$ vs. OxLDL treated alone). The cells were then pre-incubated with AG1478 followed by incubation with OxLDL and meprinα, and ROS production was also reversed ($P < 0.01$ vs. OxLDL treated with meprinα). In addition, incubation of OxLDL and meprinα after EGFR inhibition significantly decreased ROS production, which is similar to the effect which occurs when OxLDL and AG1478 were co-cultured. These findings suggest that OxLDL/meprinα-induced ROS production was dependent upon activation of EGFR.

EGFR is a transmembrane protein consisting of an extracellular ligand-binding domain to which EGFR ligands bind for activation.[26] To study which ligands are crucial in regulating OxLDL-mediated production of ROS, J774A.1 cells were pre-incubated with a mixture of EGFR agonist-neutralizing antibodies [anti-TGFα (10 μg), anti-EGF (20 μg), anti-HB-EGF (10 μg) for 2 h] before culture with OxLDL. As shown in *Figure 4D*, OxLDL-mediated production of ROS was blocked by a mixture of antibodies ($P < 0.01$ vs. OxLDL treated alone). Macrophages were then pre-incubated with anti-TGFα, anti-EGF, or anti-HB-EGF antibody, followed by incubation with OxLDL. The neutralizing antibodies of HB-EGF abolished the OxLDL-induced increase in ROS and EGFR activation by 66.6 ± 10.1% and 72.5 ± 9.7%, respectively ($P < 0.01$ vs. OxLDL treated

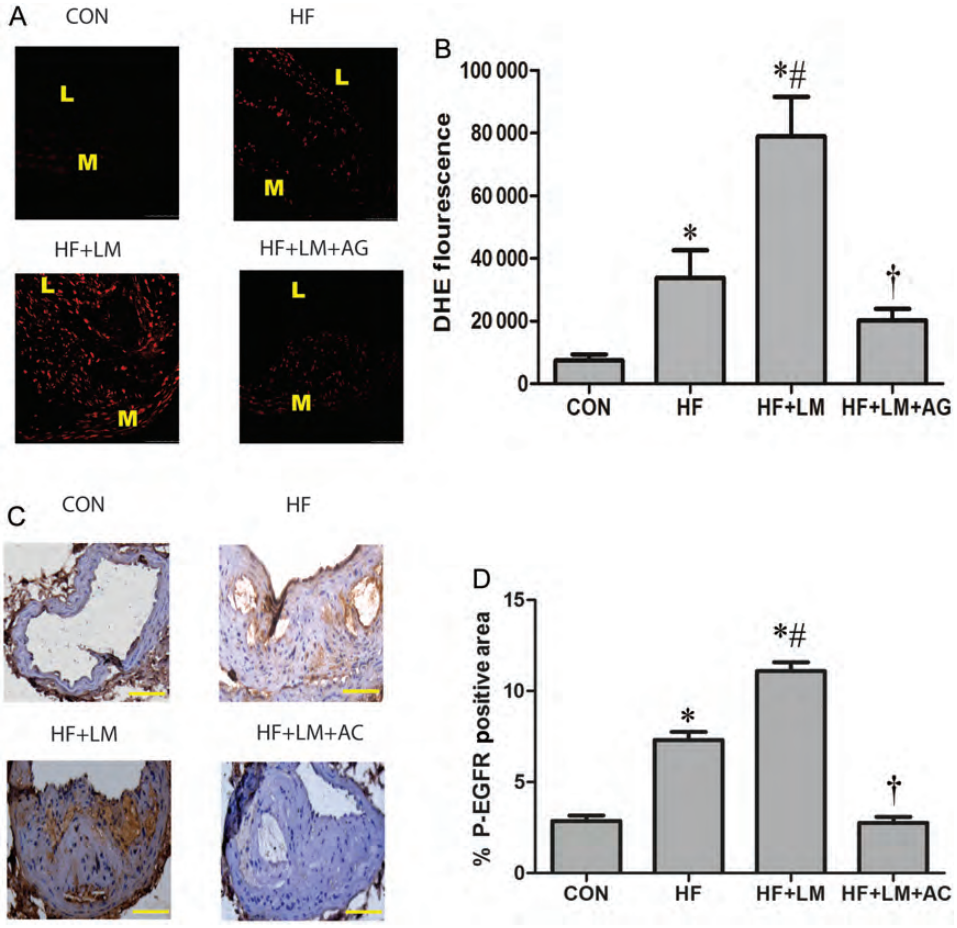

Figure 3 Meprinα regulates *in situ* ROS production and increases the expression of phosphor-EGFR in atherosclerotic plaques. (*A*) Representative DHE fluorescence images of atherosclerosis lesions in mice administered *L-meprinα* with or without AG1478. L, lumen; M, media ($n = 8–10$, bar = 75 μm). (*B*) Quantitative data in the graph represent DHE fluorescence intensity determined by IPP 6.0. *$P < 0.01$ vs. **CON,** $^{\#}P < 0.01$ vs. **HF**, and $^{\dagger}P < 0.01$ vs. **HF + LM.** (*C* and *D*) Representative immunohistochemistry images (*C*) showing expression of phosphor-EGFR in atherosclerotic lesions and (*D*) percentage of phosphor-EGFR-positive areas ($n = 6$, bar = 100). *$P < 0.01$ vs. **CON,** $^{\#}P < 0.01$ vs. **HF**, and $^{\dagger}P < 0.01$ vs. **HF + LM.**

alone, *Figures 4E* and *5A*); however, the neutralizing antibodies of EGF and TGFα had no effect on ROS production ($P > 0.05$ vs. oxLDL treated alone, *Figure 4E*).

To determine whether or not meprinα-mediated EGFR activation is involved in the OxLDL-induced increase in ROS production, macrophages were pre-incubated with actinonin or meprinα siRNA, followed by incubation with OxLDL. Phosphorylation of EGFR triggered by OxLDL was significantly reversed by actinonin or meprinα siRNA ($P < 0.01$ vs. OxLDL treated alone, *Figure 5B*). Along with OxLDL, recombinant mouse meprinα led to HB-EGF release ($P < 0.01$ vs. control, *Figure 5C*). Then, macrophages were pre-incubated with actinonin or meprinα siRNA followed by incubation with OxLDL, and the release of HB-EGF was significantly reversed ($P < 0.01$ vs. OxLDL treated alone, *Figure 5D*).

3.5 Involvement of the PI3K/Rac1/P38MAPK pathway in OxLDL-mediated induction of ROS production

To determine whether or not MAPK activation [p38, extracellular signal-regulated kinases (ERK), and c-Jun N-terminal kinases (JNK)] plays a part in OxLDL-induced ROS production, macrophages were pre-incubated with SP600125 (JNK inhibitor, 100 μmol/L), SB203580 (p38 inhibitor, 20 μmol/L), or PD98059 (ERK inhibitor, 50 μmol/L) for 1 h, followed by incubation with OxLDL. Pre-treatment with SB203580 prevented the production of ROS, whereas incubation with SP600125 or PD98059 had no effect (*Figure 6A*, Supplementary material online, *Figure S4*). Next, we determined whether OxLDL activated p38 in macrophages. Upon OxLDL stimulation, the activity of p38 significantly increased, as detected by western blot (*Figure 6B*); however, when pre-incubated with actinonin or meprinα siRNA, OxLDL-induced phosphorylation of p38 was significantly reversed (*Figure 6B*).

Moreover, a previous report demonstrated that activation of Rac1 GTPase is involved in OxLDL-stimulated ROS production.[27] To understand the OxLDL-induced signalling relationship between Rac1 and p38, J774A.1 cells were pre-incubated with the Rac1 inhibitor, EHT1864 (10 μmol/L), for 4 h. The results of p38 activity in cells pre-incubated with EHT1864 and treated with OxLDL suggest a significantly lower activity of p38 compared with cells treated with OxLDL alone (*Figure 6C*).

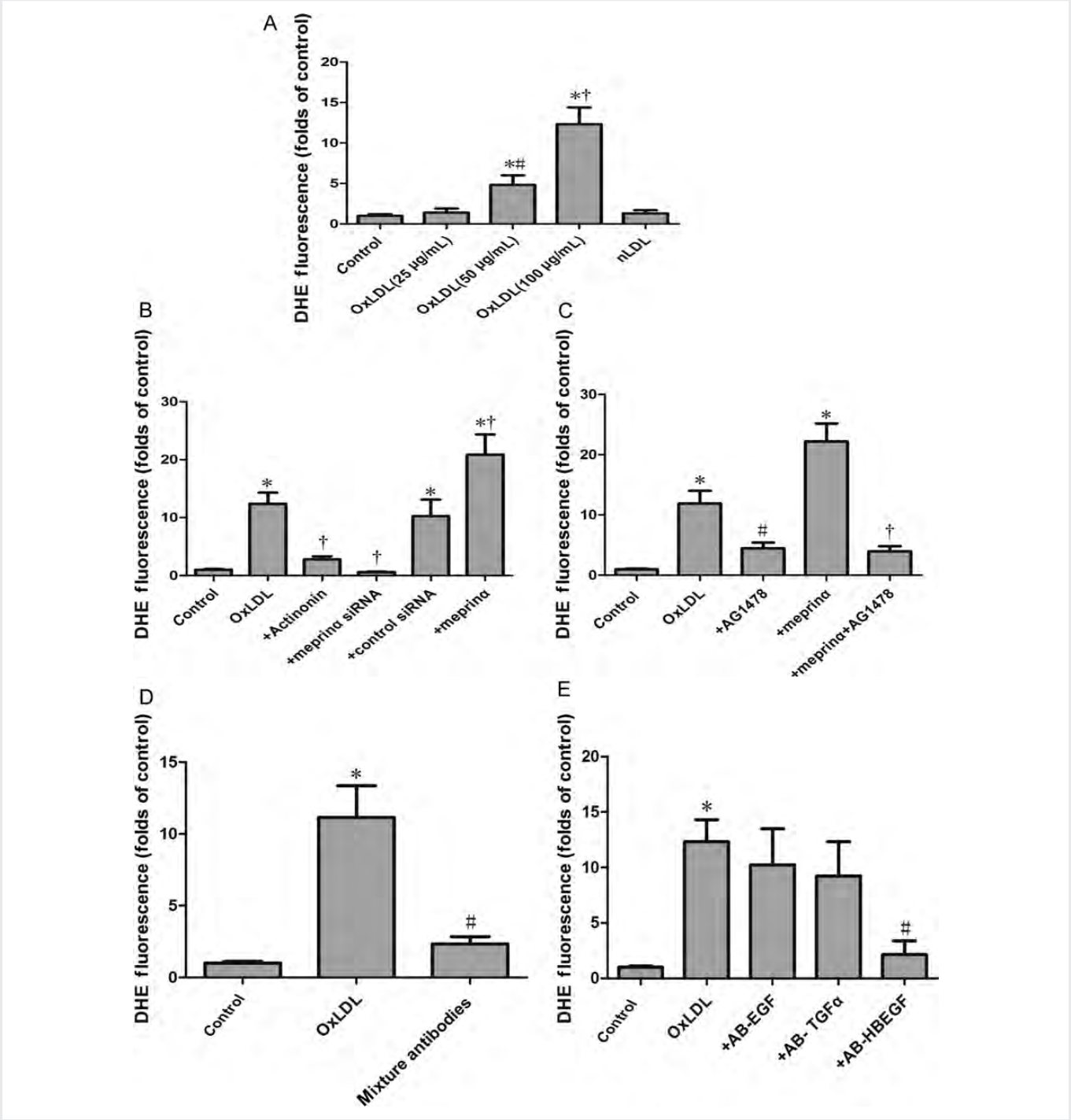

Figure 4 Regulation of OxLDL-induced ROS production in J774A.1 macrophages. Quantitative data in the graph represent the mean ± SEM of relative DHE fluorescence of three to six separate experiments. (*A*) OxLDL-induced production of ROS in macrophages in a concentration-dependent manner. $^{*}P < 0.01$ vs. control, $^{\#}P < 0.01$ vs. OxLDL (25 μg/mL), and $^{\dagger}P < 0.01$ vs. OxLDL (100 μg/mL). (*B*) Role of meprinα in OxLDL-induced ROS production. $^{*}P < 0.01$ vs. control, $^{\dagger}P < 0.01$ vs. OxLDL. (*C*) The EGFR-specific inhibitor, AG1478, suppressed OxLDL- and meprinα-stimulated ROS production. $^{*}P < 0.01$ vs. control, $^{\#}P < 0.01$ vs. OxLDL, and $^{\dagger}P < 0.01$ vs. OxLDL+meprinα. (*D*) Mixture of neutralizing antibodies of EGFR ligands significantly suppressed OxLDL-induced ROS production. $^{*}P < 0.01$ vs. control, $^{\#}P < 0.01$ vs. OxLDL. (*E*) Neutralizing antibodies of HB-EGF suppressed OxLDL-stimulated ROS production. $^{*}P < 0.01$ vs. control, $^{\#}P < 0.01$ vs. OxLDL.

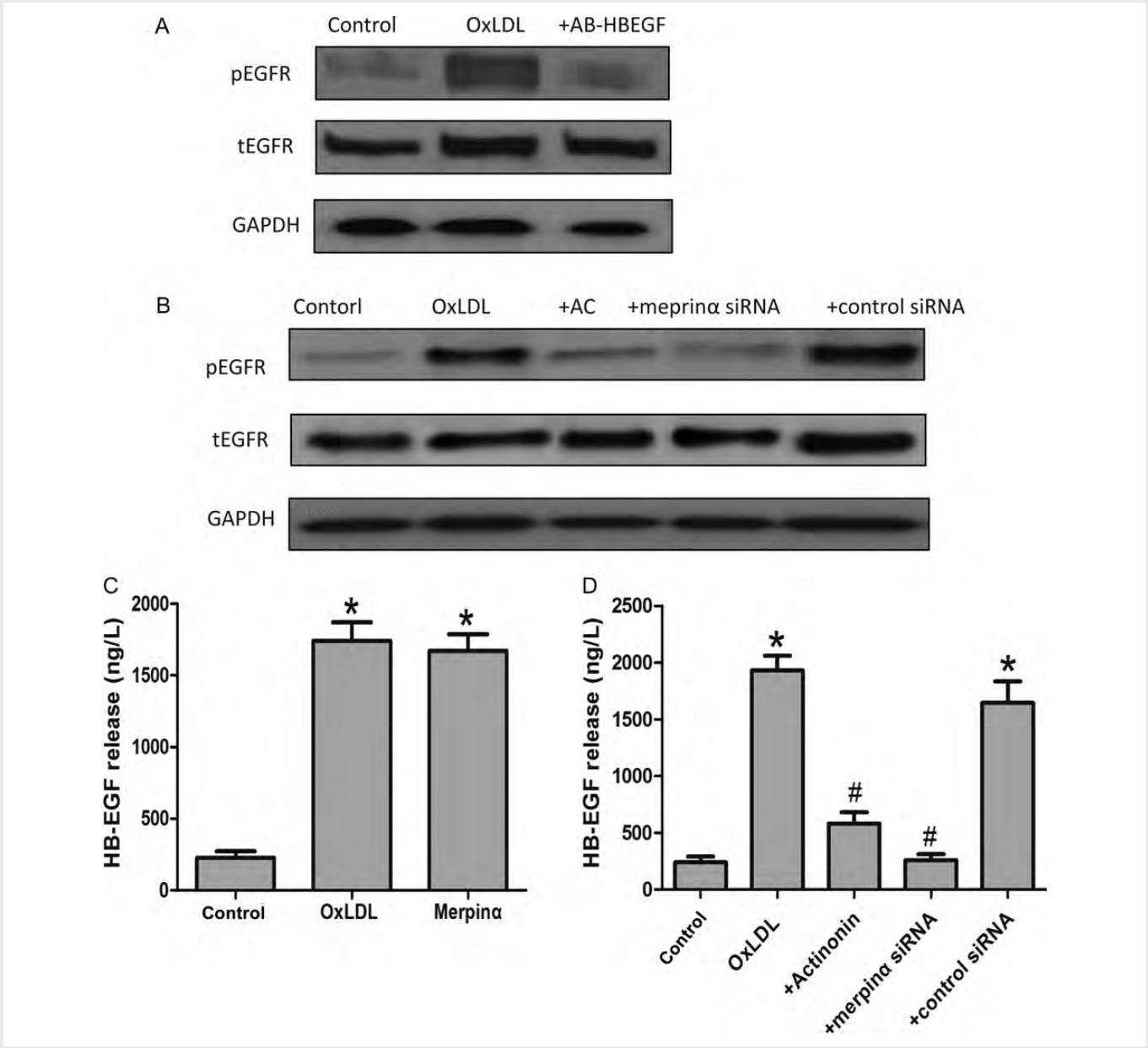

Figure 5 Inhibition of meprinα suppresses transactivation of EGFR and production of HB-EGF. Quantitative data in the graph represent the mean ± SEM of three to six separate experiments. (*A*) Neutralizing antibodies of HBEGF suppresses oxLDL-stimulated phosphorylation of EGFR. The blot is representative of three experiments. (*B*) J774A.1 cells were transfected with control siRNA, meprinα siRNA, and actinonin, followed by incubation with oxLDL for 1 h. Actinonin and meprinα siRNA significantly decreased oxLDL-stimulated activation of EGFR. The blot is representative of three experiments. (*C*) Meprinα along with oxLDL induced HB-EGF release. $^{*}P < 0.01$ vs. control group. (*D*) Actinonin and meprinα siRNA significantly decreased OxLDL-stimulated HB-EGF release. $^{*}P < 0.01$ vs. control, $^{\#}P < 0.01$ vs. OxLDL.

Phosphoinositide 3-kinase (PI3K) is known to participate in the signalling events leading to ROS production and Rac1 activation in the metalloprotease-mediated transactivation of EGFR. J774A.1 cells were pre-treated with or without wortmannin (an inhibitor of PI3K, 1 μmol/L) for 1 h, followed by incubation with OxLDL, and then the activity of p38 was examined. As shown in *Figure 6D*, in the absence of wortmannin, OxLDL induced p38 activity by approximately nine-fold when compared with control cells. Pre-treatment of cells with wortmannin resulted in failed induction of p38 activity by OxLDL. These results suggest that PI3K is involved in OxLDL-mediated p38 activity. In addition, macrophages were pre-treated with or without wortmannin, followed by incubation with OxLDL, and then the activity of Rac1 was examined. Wortmannin significantly decreased OxLDL-induced Rac1 activity in macrophages (*Figure 6E*), suggesting that PI3K functions upstream of Rac1.

3.6 Inhibition of the meprinα–EGFR pathway suppresses PI3K-mediated activation of Akt

To determine whether or not meprinα transactivation of EGFR is involved in ROS production by PI3K activation, macrophages were

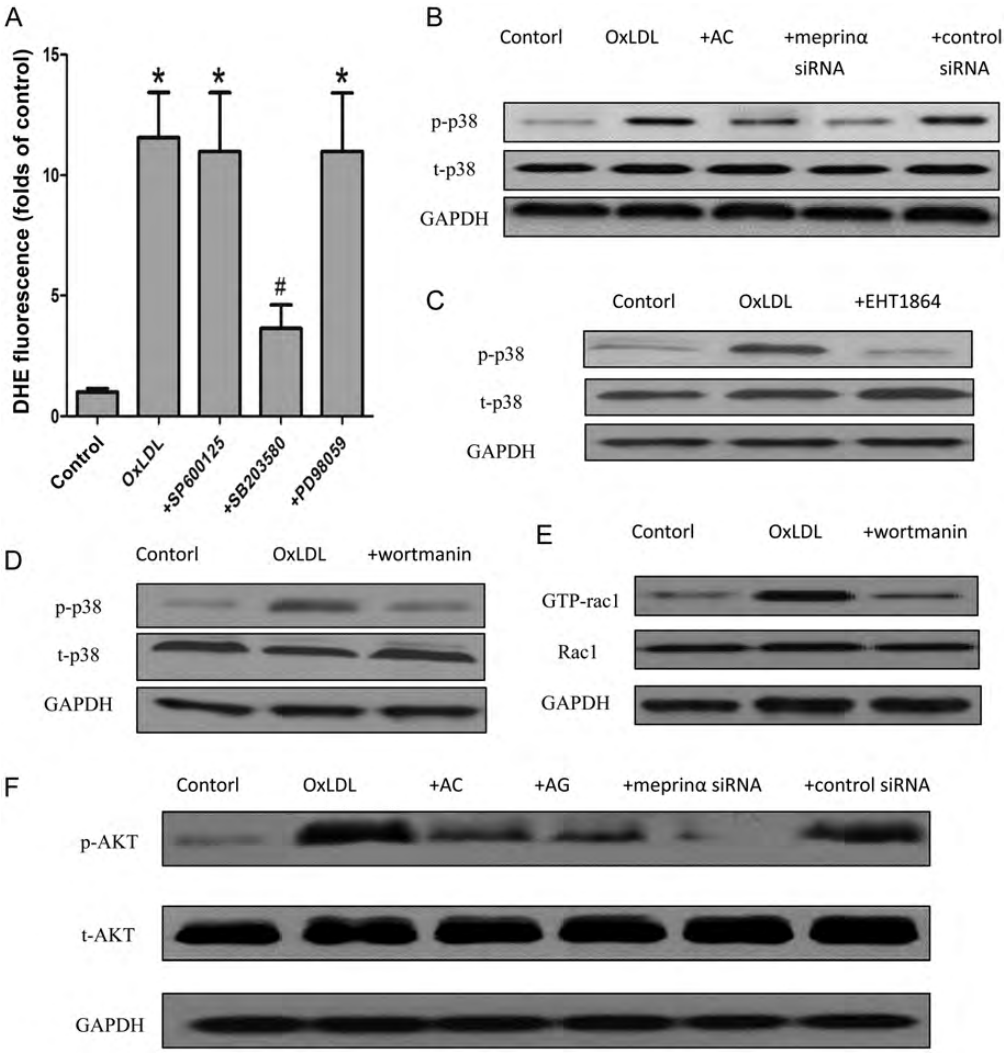

Figure 6 Role of PI3K-Rac1-P38 signalling in OxLDL-induced ROS production in J774A.1 macrophages. Quantitative data in the graph represent the mean ± SEM of three to six separate experiments. The blot is representative of three experiments. (*A*) Effects of MAPK signalling inhibitors on ROS production. $^{*}P < 0.01$ vs. control, $^{\#}P < 0.01$ vs. OxLDL. (*B*) Inhibition of p38 activity by meprinα siRNA and actinonin. (*C*) Phosphorylation of p38 was significantly suppressed by Rac1 inhibitor. (*D*) PI3K inhibitor significantly decreased p38 activity. (*E*) Expression of GTP-Rac1 in OxLDL-treated macrophages with or without PI3K inhibitor. (*F*) Inhibition of meprinα and EGFR signalling decreased OxLDL-stimulated phosphorylation of Akt.

cultured with OxLDL in the presence or absence of actinonin and AG1478. PI3K activation was determined by the phosphorylation of Akt at Ser473 (a PI3K substrate). Stimulation of OxLDL significantly increased the phosphorylation of Akt, which was blunted in the presence of actinonin and AG1478 (*Figure 6F*). In addition, meprinα siRNA also significantly prevented the increase in phosphorylation of Akt by OxLDL (*Figure 6F*).

4. Discussion

In the present study, we provide three novel findings regarding meprinα-mediated atherosclerosis. First, meprinα is a positive regulator of the formation of atherosclerotic plaques. Second, meprinα plays an essential part in ox-LDL-mediated ROS production and EGFR transactivation in macrophages, which leads to formation of atherosclerotic plaques. Third, we also showed that the release of the EGFR ligand, HB-EGF, is an important mediator of EGFR transactivation by meprinα, and the PI3K/Rac1/P38 signalling pathway is also involved in meprinα-mediated ROS production.

Macrophages secrete several classes of neutral extracellular proteases, including serine proteases, cathepsins, and metalloproteinases.[28,29] Accumulated evidence has demonstrated that members of the metalloproteinase family have important roles in atherosclerosis.[30,31] Astacins are a subfamily of the metzincin superfamily of metalloproteinases. Meprins are the only astacin proteinases that function on the membrane and extracellularly because meprins can be membrane-bound or secreted.[18] In health, meprins are highly regulated at the transcriptional and post-translational levels. Meprins localize to specific membranes or extracellular spaces, and the main function of meprins is to hydrolyze biologically active peptides, cytokines, extracellular matrix (ECM) proteins, and cell-surface proteins. Recently, the MEP1A gene, which encodes the α-subunit of metalloproteinase meprin, has been shown to be related

to the inflammatory process;[19,21,23] however, the precise biological mechanisms have not been verified.

Metalloproteases have been implicated in the ectodomain shedding of cell surface proteins, including EGFR. The matrix metalloproteinases, by shedding mature growth factors, then bind to EGFR and phosphorylate tyrosine kinase.[32] A recent study reported that dysintegrin and metalloproteinases can activate EGFR by switching HB-EGF into an active form.[30] The role of meprinα in ligand processing for EGFR activation has also been described in epidermal cells; it appears that metalloprotease induced-transactivation of EGFR is dependent upon various upstream ligands in different cell types and stimuli.[23,24] Our results demonstrated that there was endogenous meprinα expression in atherosclerotic plaques. We then showed that meprinα can exaggerate OxLDL-induced EGFR activation and ROS production by promoting the release of soluble HB-EGF *ex vivo*. These data suggest that the meprinα–EGFR axis influences atherosclerosis formation in an oxidative stress-dependent pathway.

Previous studies have demonstrated that MAPK pathways are involved in the ROS release in macrophages.[33,34] In the present experiments, when pre-incubated with ERK1/2 or JNK inhibitor, ROS release did not show a significant reduction in macrophages. Conversely, the p38 inhibitor, SB203580, significantly attenuated OxLDL-induced ROS production. Furthermore, because actinonin and meprinα siRNA attenuated phosphorylation of p38, it was suggested that meprinα is the upstream kinase of p38.

Having established that p38 activation is involved in OxLDL/meprinα-mediated induction of ROS, it has also been shown that PI3K is involved in the matrix metalloproteinase-EGFR increase in ROS release,[35] but the downstream components of this signalling mechanism in macrophages have not been clearly identified. We showed that the inhibition of meprinα by actinonin and siRNA or EGFR by AG1478 significantly attenuated phosphorylation of Akt, a substrate of PI3K, and we also showed that the inhibition of PI3K by wortmanin reversed the OxLDL-induced activation of p38 and Rac1, suggesting that PI3K functions as an upstream signal to p38 and Rac1 in macrophages.

Akt, a serine/threonine kinase, is a direct downstream signal of PI3K. Akt can be modified by multiple intracellular signalling molecules and acts as a transducer for many pathways initiated by growth factor receptor-activated PI3K.[36] Indeed, our data demonstrated that OxLDL-activated meprinα causes activation of PI3K downstream of EGFR, as detected by the increased levels of phospho-Akt. Rac1, a Rho family GTPase, participates in the regulation of various cellular functions, such as production of oxygen radicals, through activation of a number of signalling pathways, including ERK, p38, and NF-κB.[37,38] In J774A.1 macrophages, inhibition of Rac1 significantly reduced the phosphorylation of p38, suggesting that Rac1 acts upstream of p38 and mediates OxLDL-induced oxidative stress. Taken together, these data suggest that meprinα activates the PI3K/Rac1/P38 pathway through transactivation of EGFR to induce ROS production in OxLDL-treated macrophages.

In summary, we have demonstrated that increased meprinα levels induce oxidative stress in macrophages, which may represent an important mechanism by which meprinα promotes atherosclerosis. These effects of meprinα are mediated through HB-EGF-dependent activation of EGFR and its downstream signal. Our findings complement the work of others investigating the mechanism of metalloproteinase transactivation of the EGFR, which contributes to atherosclerosis.

Supplementary material

Supplementary material is available at *Cardiovascular Research* online.

Acknowledgements

We appreciate the technical assistance of Meng-Yang Deng, Hua-Li Kang, and De-Ying Chen. We also thank Dr Liu Hong for giving us the high-fat diet for apoE$^{-/-}$ mice.

Conflict of interest: none declared.

Funding

This work was supported by a grant from the National Natural Science Foundation of China (No.81000132) and a grant from the special fund of Chongqing Key Laboratory (CSTC) of the Institute of Cardiovascular Science in XinQiao Hospital.

References

1. Glass CK, Witztum JL. Atherosclerosis: the road ahead. *Cell* 2001;**104**:503–516.
2. Asmis R, Begley JG. Oxidized LDL promotes peroxide-mediated mitochondrial dysfunction and cell death in human macrophages: a caspase-3-independent pathway. *Circ Res* 2003;**92**:e20–e29.
3. Assinger A, Koller F, Schmid W, Zellner M, Koller E, Volf I. Hypochlorite-oxidized LDL induces intraplatelet ROS formation and surface exposure of CD40L—a prominent role of CD36. *Atherosclerosis* 2010;**213**:129–134.
4. Moore KJ, Freeman MW. Scavenger receptors in atherosclerosis: beyond lipid uptake. *Arterioscler Thromb Vasc Biol* 2006;**26**:1702–1711.
5. Shi Y, Cosentino F, Camici GG, Akhmedov A, Vanhoutte PM, Tanner FC *et al*. Oxidized low-density lipoprotein activates p66Shc via lectin-like oxidized low-density lipoprotein receptor-1, protein kinase C-beta, and c-Jun N-terminal kinase kinase in human endothelial cells. *Arterioscler Thromb Vasc Biol* 2011;**31**:2090–2097.
6. Bedel A, Negre-Salvayre A, Heeneman S, Grazide MH, Thiers JC, Salvayre R *et al*. E-cadherin/beta-catenin/T-cell factor pathway is involved in smooth muscle cell proliferation elicited by oxidized low-density lipoprotein. *Circ Res* 2008;**103**:694–701.
7. Mukai E, Kume N, Hayashida K, Minami M, Yamada Y, Seino Y *et al*. Heparin-binding EGF-like growth factor induces expression of lectin-like oxidized LDL receptor-1 in vascular smooth muscle cells. *Atherosclerosis* 2004;**176**:289–296.
8. Auge N, Garcia V, Maupas-Schwalm F, Levade T, Salvayre R, Negre-Salvayre A. Oxidized LDL-induced smooth muscle cell proliferation involves the EGF receptor/PI-3 kinase/Akt and the sphingolipid signaling pathways. *Arterioscler Thromb Vasc Biol* 2002;**22**:1990–1995.
9. DeYulia GJ Jr., Carcamo JM, Borquez-Ojeda O, Shelton CC, Golde DW. Hydrogen peroxide generated extracellularly by receptor-ligand interaction facilitates cell signaling. *Proc Natl Acad Sci USA* 2005;**102**:5044–5049.
10. Lee SJ, Kim CE, Seo KW, Kim CD. HNE-induced 5-LO expression is regulated by NF-{kappa}B/ERK and Sp1/p38 MAPK pathways via EGF receptor in murine macrophages. *Cardiovasc Res* 2010;**88**:352–359.
11. Shah BH, Catt KJ. Matrix metalloproteinase-dependent EGF receptor activation in hypertension and left ventricular hypertrophy. *Trends Endocrinol Metab* 2004;**15**:241–243.
12. Kimura S, Zhang GX, Nishiyama A, Shokoji T, Yao L, Fan YY *et al*. Mitochondria-derived reactive oxygen species and vascular MAP kinases: comparison of angiotensin II and diazoxide. *Hypertension* 2005;**45**:438–444.
13. Zhang H, Chalothorn D, Jackson LF, Lee DC, Faber JE. Transactivation of epidermal growth factor receptor mediates catecholamine-induced growth of vascular smooth muscle. *Circ Res* 2004;**95**:989–997.
14. Higashiyama S, Iwabuki H, Morimoto C, Hieda M, Inoue H, Matsushita N. Membrane-anchored growth factors, the epidermal growth factor family: beyond receptor ligands. *Cancer Sci* 2008;**99**:214–220.
15. Berk BC. Vascular smooth muscle growth: autocrine growth mechanisms. *Physiol Rev* 2001;**81**:999–1030.
16. Saito Y, Berk BC. Transactivation: a novel signaling pathway from angiotensin II to tyrosine kinase receptors. *J Mol Cell Cardiol* 2001;**33**:3–7.
17. Zwick E, Hackel PO, Prenzel N, Ullrich A. The EGF receptor as central transducer of heterologous signalling systems. *Trends Pharmacol Sci* 1999;**20**:408–412.
18. Sterchi EE, Stocker W, Bond JS. Meprins, membrane-bound and secreted astacin metalloproteinases. *Mol Aspects Med* 2008;**29**:309–328.
19. Yura RE, Bradley SG, Ramesh G, Reeves WB, Bond JS. Meprin A metalloproteases enhance renal damage and bladder inflammation after LPS challenge. *Am J Physiol Renal Physiol* 2009;**296**:F135–F144.
20. Sun Q, Jin HJ, Bond JS. Disruption of the meprin alpha and beta genes in mice alters homeostasis of monocytes and natural killer cells. *Exp Hematol* 2009;**37**:346–356.

21. Gao P, Si LY. Meprin-alpha metalloproteases enhance lipopolysaccharide-stimulated production of tumour necrosis factor-alpha and interleukin-1beta in peripheral blood mononuclear cells via activation of NF-kappaB. *Regul Pept* 2010;**160**:99–105.
22. Gao P, Guo RW, Chen JF, Chen Y, Wang H, Yu Y *et al*. A meprin inhibitor suppresses atherosclerotic plaque formation in ApoE-/- mice. *Atherosclerosis* 2009;**207**:84–92.
23. Bergin DA, Greene CM, Sterchi EE, Kenna C, Geraghty P, Belaaouaj A *et al*. Activation of the epidermal growth factor receptor (EGFR) by a novel metalloprotease pathway. *J Biol Chem* 2008;**283**:31736–31744.
24. Cosgrove S, Chotirmall SH, Greene CM, McElvaney NG. Pulmonary proteases in the cystic fibrosis lung induce interleukin 8 expression from bronchial epithelial cells via a heme/meprin/epidermal growth factor receptor/Toll-like receptor pathway. *J Biol Chem* 2011;**286**:7692–7704.
25. Cowen T, Haven AJ, Burnstock G. Pontamine sky blue: a counterstain for background autofluorescence in fluorescence and immunofluorescence histochemistry. *Histochemistry* 1985;**82**:205–208.
26. Schwenk JM, Poetz O, Zeillinger R, Joos TO. A miniaturized ligand binding assay for EGFR. *Int J Proteomics* 2012;**2012**:247059.
27. Dentelli P, Rosso A, Zeoli A, Gambino R, Pegoraro L, Pagano G *et al*. Oxidative stress-mediated mesangial cell proliferation requires RAC-1/reactive oxygen species production and beta4 integrin expression. *J Biol Chem* 2007;**282**:26101–26110.
28. Newby AC. Metalloproteinase expression in monocytes and macrophages and its relationship to atherosclerotic plaque instability. *Arterioscler Thromb Vasc Biol* 2008; **28**:2108–2114.
29. Dollery CM, Libby P. Atherosclerosis and proteinase activation. *Cardiovasc Res* 2006; **69**:625–635.
30. Lee S, Springstead JR, Parks BW, Romanoski CE, Palvolgyi R, Ho T *et al*. Metalloproteinase processing of HBEGF is a proximal event in the response of human aortic endothelial cells to oxidized phospholipids. *Arterioscler Thromb Vasc Biol* 2012;**32**: 1246–1254.
31. Orbe J, Barrenetxe J, Rodriguez JA, Vivien D, Orset C, Parks WC *et al*. Matrix metalloproteinase-10 effectively reduces infarct size in experimental stroke by enhancing fibrinolysis via a thrombin-activatable fibrinolysis inhibitor-mediated mechanism. *Circulation* 2011;**124**:2909–2919.
32. Prenzel N, Zwick E, Daub H, Leserer M, Abraham R, Wallasch C *et al*. EGF receptor transactivation by G-protein-coupled receptors requires metalloproteinase cleavage of proHB-EGF. *Nature* 1999;**402**:884–888.
33. Yu JY, Zheng ZH, Son YO, Shi X, Jang YO, Lee JC. Mycotoxin zearalenone induces AIF- and ROS-mediated cell death through p53- and MAPK-dependent signaling pathways in RAW264.7 macrophages. *Toxicol In Vitro* 2011;**25**:1654–1663.
34. Giovannini C, Vari R, Scazzocchio B, Sanchez M, Santangelo C, Filesi C *et al*. OxLDL induced p53-dependent apoptosis by activating p38MAPK and PKCdelta signaling pathways in J774A.1 macrophage cells. *J Mol Cell Biol* 2011;**3**:316–318.
35. Nagareddy PR, Chow FL, Hao L, Wang X, Nishimura T, MacLeod KM *et al*. Maintenance of adrenergic vascular tone by MMP transactivation of the EGFR requires PI3K and mitochondrial ATP synthesis. *Cardiovasc Res* 2009;**84**:368–377.
36. Franke TF, Kaplan DR, Cantley LC, Toker A. Direct regulation of the Akt proto-oncogene product by phosphatidylinositol-3,4-bisphosphate. *Science* 1997; **275**:665–668.
37. Woo CH, Kim JH. Rac GTPase activity is essential for lipopolysaccharide signaling to extracellular signal-regulated kinase and p38 MAP kinase activation in rat-2 fibroblasts. *Mol Cells* 2002;**13**:470–475.
38. Chen BC, Kang JC, Lu YT, Hsu MJ, Liao CC, Chiu WT *et al*. Rac1 regulates peptidoglycan-induced nuclear factor-kappaB activation and cyclooxygenase-2 expression in RAW 264.7 macrophages by activating the phosphatidylinositol 3-kinase/Akt pathway. *Mol Immunol* 2009;**46**:1179–1188.